JOURNAL OF MATERIALS SCIENCE 38 (2003) 4451–4460

High throughput methods for polymer nanocomposites research: Extrusion, NMR characterization and flammability property screening

J. W. GILMAN†
Fire Research Division, National Institute of Standards and Technology, Gaithersburg, MD, USA
E-mail: jeffrey.gilman@nist.gov

S. BOURBIGOT*
Laboratoire de Génie et Matériaux Textiles (GEMTEX), Ecole Nationale des Arts et Industries Textiles (ENSAIT), ROUBAIX, France

J. R. SHIELDS, M. NYDEN, T. KASHIWAGI, R. D. DAVIS
Fire Research Division, National Institute of Standards and Technology, Gaithersburg, MD, USA

D. L. VANDERHART
Polymers Division, National Institute of Standards and Technology, Gaithersburg, MD, USA

W. DEMORY
Fire Research Division, National Institute of Standards and Technology, Gaithersburg, MD, USA

C. A. WILKIE
Department of Chemistry, Marquette University, Milwaukee, WI, USA

A. B. MORGAN, J. HARRIS
Corporate R&D, The Dow Chemical Co., Midland, MI, USA

R. E. LYON*
Fire Research Branch, Federal Aviation Administration Technical Center, Atlantic City, NJ, USA

A large number of parameters influence polymer-nanocomposite performance and developing a detailed understanding of these materials involves investigation of a large volume of the associated multi-dimensional property space. This multi-dimensional parameter space for polymer-nanocomposites consists of the obvious list of different material types under consideration, such as "polymer" and "nano-additive," but also includes interphase surface chemistry, and processing conditions. This article presents combinatorial library design and high-throughput screening methods for polymer nanocomposites intended as flame-resistant materials. Here, we present the results of using a twin-screwn extruder to create composition-gradient library strips of polymer nanocomposites that are screened with a solid-state NMR method to rapidly evaluate the optimal processing conditions for achieving nanocomposite dispersion. In addition, we present a comparison of a new rapid Cone calorimetry method to conventional Cone calorimetry and to the gradient heat-flux flame spread method. © *2003 Kluwer Academic Publishers*

1. Introduction

Several, recent, revolutionary advances in combinatorial (or high throughput, HT) polymer science have appeared in the literature, which significantly accelerate the rate of data generation [1–6]. Although these new HT approaches may in part have been inspired by the similar application of HT concepts in the catalyst field, the development of these methods for polymer

†Corresponding author.
*NIST guest researcher.

0022–2461

research required new techniques be created specifically for the unique issues associated with polymers. These elegant advances are a challenge placed before the polymer community to create new more efficient analytical, synthetic, processing, and characterization methods useful for the study of other polymer problems.

The goal of our research program is the development of a system of HT methods for rapid, detailed study of polymer nanocomposites. Whenever possible we attempt to keep the cost of the approach in mind and use standard commercially available equipment.

An additional goal of our research focuses on the development of fundamental structure-property relations for polymer nanocomposites. Our primary interest is to develop an understanding of the governing, fundamental, mechanisms behind the enhanced mechanical properties and improved flammability properties of nanocomposites.

Polymer nanocomposites are prepared by mixing a polymer (or monomer) with some dissimilar material, or additive, that has one or more dimensions on the nanometer scale. Over the last few decades, a wide variety of materials and synthesis approaches have been developed that allow molecular-level control over the design and structure of nanocomposite materials. Nanocomposites have been prepared by sol gel methods [7], by *in situ* polymerization routes, and by using simple compounding methods [8]. All of these approaches share a common theme; the intermingling, on the nanometer scale, of dissimilar materials for the purpose of creating new materials with properties not available from either of the component pure materials. For example, simple organic polymers modified with layered silicates [9, 10] have been prepared with improved heat distortion temperatures, twice the modulus, a factor of ten lower permeability of gases and solvents, improved thermal stability, a 4-fold lower flammability [11–15], enhanced ablative performance [16], and reduced rates of degradation in space [17]. All these attributes derive from incorporation of only 5 to 10% (mass fraction) of the layered silicate, and only occur if the surface-area between the two phases is very high, i.e., the particle size of the additive is on the nanometer scale and the degree of phase mixing is homogeneous on the nanometer scale. In other words, the fraction of material in an "interphase" must be high. Other types of nanocomposites that show similar enhanced properties, as long as the same conditions are met, are polyoligosilsesquioxane, POSS, materials blended or copolymerized with various polymers [18], sol-gel hybrid materials [19], nano-silica composites [20], and polymer-nanocomposites based on graphite [21, 22] and carbon nano-tubes [23, 24].

From this brief introduction to polymer-nanocomposites it should be evident that there are a large number of parameters, which influence polymer-nanocomposite performance; thus, to develop a detailed understanding of these materials a large volume of the associated multi-dimensional property space should be investigated.

The multi-dimensional parameter space for polymer-nanocomposites, shown in Table I, consists of the obvious list of different material types under consideration, such as "polymer" and "nano-additive." All of these materials must be miscible with one another so that a nanocomposite can form, and so that there is a strong stabilizing interaction at the interphase between the two dissimilar materials. This is essential both for the phase stability of the nanocomposite, and for optimal physical properties. These requirements introduce the next parameter, "surface chemistry." Control of surface chemistry is most often accomplished, in layered silicate nanocomposites, by modification of the inorganic surface with an organophillic reagent, such as an alkyl ammonium, or a chelating agent. In POSS materials, many different functionalities can be incorporated directly into the structure. While this means that no additional "surface" treatment is required, there are still a large number of possible POSS materials which need to be evaluated to obtain the optimal property improvement for a specific application [25].

As with layered-silicates, both carbon-nanotubes and silica nano-particles may require secondary functionalization to render them miscible with a variety of polymers. This brings us to the very critical parameter, "processing conditions." The optimal processing conditions for a given nanocomposite system will depend on complex interactions with the previous three parameters. We have found that careful control of processing conditions is critical both to the preparation of a nanocomposite, and also to preventing degradation of the nanocomposite during processing [26]. For the purpose of considering combinations of

TABLE I Multi-dimensional parameter space for polymer-nanocomposites

Polymer[a]	Nano-additive	Surface chemistry	Processing conditions	Conventional additives	Flame retardant
PE	Layered-silicate	Alkylammonium	Temperature	Processing-stabilizers	Phosphorus Halogen
PP	POSS	Imidazolium	Shear	UV-stabilizers	Silicon-based
PS	Carbon-nanotubes	Chelates	Residence time	Antioxidant	
PA6	Silica	Silated		Fillers	
PU		Alkyl		Pigments	
PVC		Carboxylate			
PC					
PEO					
Epoxy					
~10	~10	~10	~10	~10	~10

[a]Polyethylene (PE), polypropylene (PP), polystyrene (PS), polyamide-6 (PA-6), polyurethane (PU), polyvinyl chloride (PVC), polycarbonate (PC), polyethylene oxide (PEO).

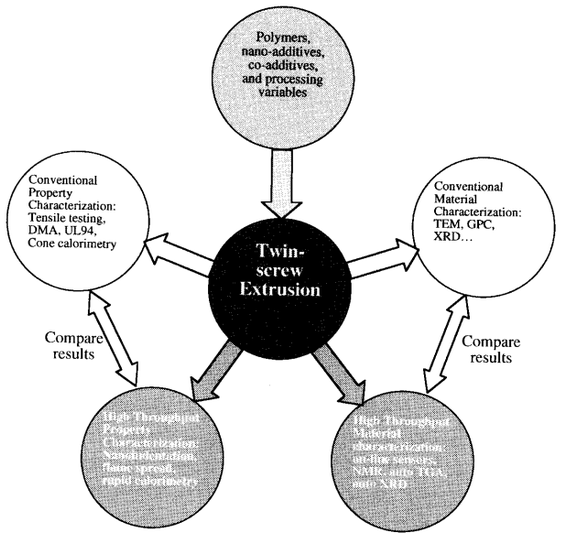

Figure 1 Schematic diagram of the high throughput (HT) methods system for rapid study of polymer nanocomposites.

nanocomposites with other "conventional additives," one also needs to include the investigation of possible synergistic and antagonistic interactions with processing and UV stabilizers, pigments, dyes, fillers and for our particular interests, flame retardant additives. This list of parameters generates on the order of 10^6 combinations or formulations worthy of investigation.

To study this property space high throughput methods must be developed for nanocomposites. Fig. 1 shows a schematic of the approach taken to develop these high throughput methods. The approach begins by considering which set of the millions of combinations of: polymers, nano-additives, co-additives and processing variables needs to be evaluated (Fig. 1, top circle). At this stage, our primary goal is to develop the HT tools; therefore a previously characterized system is chosen that will allow comparison of the results from use of the conventional characterization tools to the results from characterization using the HT tools. The role of the laboratory-scale twin-screw extruder (Fig. 2) in this HT system is that of a HT preparation tool for compounding samples (or libraries). The inherent HT nature of an extruder is derived from four important capabilities:

(1) the high mass flow rates (2–3 kg/h),
(2) the ability to automate changes in the feeders used to deliver polymer and additive,
(3) the ability to easily change the processing conditions, such as residence time and shear, and
(4) direct extrusion of the samples in the form required for subsequent characterization.

We extrude strips of samples, which are used directly in our HT evaluations (flame spread measurements, the rapid Cone tests, and nanoindentation).

While these attributes offer HT preparation of compounded nanocomposite samples, they also introduce a bottle-neck in our workflow: the characterization of the library. Nanocomposites present an especially difficult, albeit interesting, challenge in this regard. In contrast to conventional fillers and additives, where simple measurement of their concentration might suffice, characterization of nanocomposites must be done with resolution at the nano-scale. Specifically, one needs to determine the degree of mixing of the individual nano-scale particles. In addition, the effect of this nano-mixing on the overall order and morphology of the system must be determined. Traditionally this is done using transmission electron microscopy (TEM), X-ray diffraction (XRD) and other methods (small angle neutron scattering, (SANS), solid-state nuclear magnetic resonance (NMR), rheometry). These methods are not usually considered HT, although some have been converted to HT systems [27].

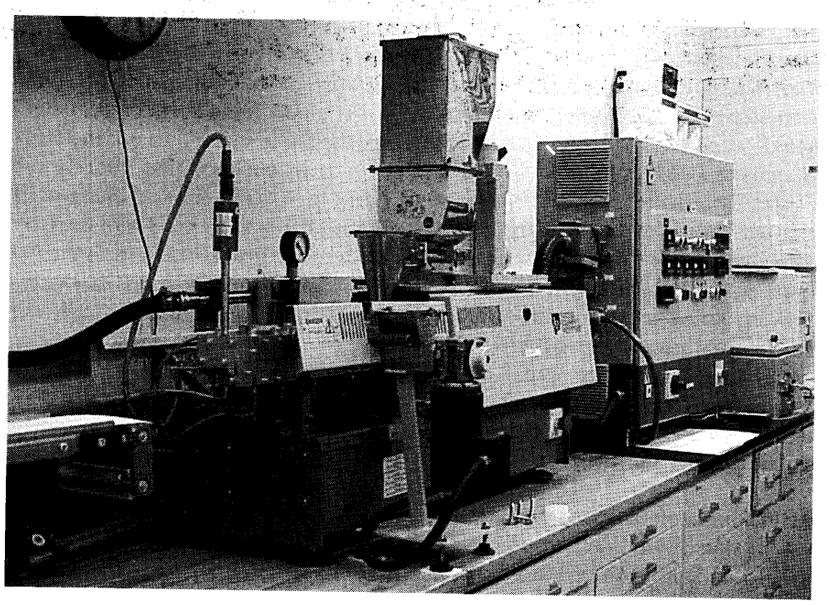

Figure 2 Photo of the twin-screw extrusion facility.

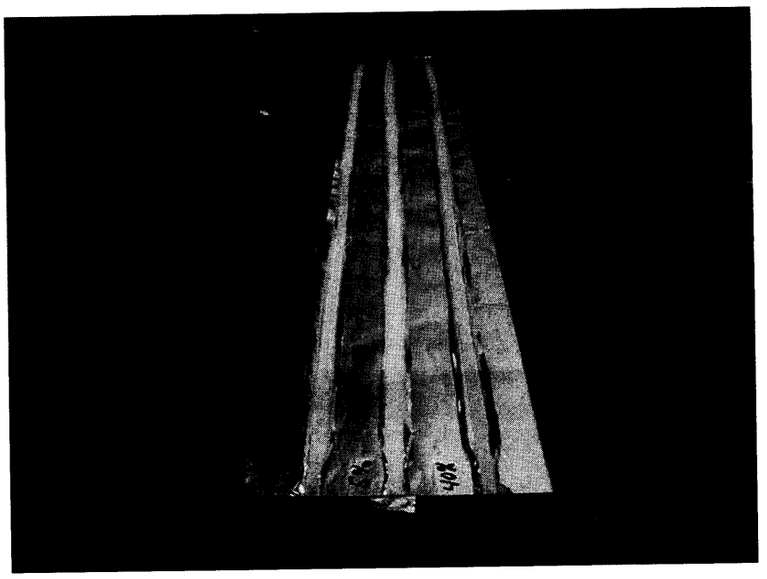

Figure 3 Extruded strips of polystyrene (PS) with various concentrations of additive.

Our recent efforts focus on removing this "characterization" bottleneck by using *in-line* sensor and *off-line* rapid characterization methods. We are developing two *in-line* tools: (1) an optical sensor [28] and (2) a dielectric sensor [29]. Both sensors are directly in-line on the extruder. The details of these sensors will be published separately. We have also developed an *off-line* solid-state NMR method for measuring the extent of nanomixing of LS polymer nanocomposites [30], some of which will be presented below. The full details of this NMR technique, and other examples of its application, will also be published separately [31]. The motivation for development of this NMR method stems from the limitations associated with TEM, i.e., the localized and qualitative nature of the images.

Once HT methods are in hand for preparing nanocomposite samples and for their characterization, the next task in the HT workflow is property characterization. Our interest in nanocomposites is focused on flammability and mechanical properties. The traditional approach to evaluating these properties often involves injection molding test coupons and property testing using standard procedures (tensile testing, dynamic mechanical analysis (DMA), flammability testing (UL94 [32], Cone Calorimeter [33]). Instead, we directly extrude the test strips, and utilize the inherent HT nature of nanoindentation for mechanical properties measurements, and new flammability characterization techniques involving measurement of flame spread, and a rapid Cone calorimetry procedure. Elsewhere, we have reported on the flame spread methods, which utilize *gradients* in either the fire environment (heat flux gradient, Fig. 5) or a gradient in the sample composition along the length of the strip [34].

Here, we present: (1) the results of using the extruder, coupled with the solid-state NMR method, to rapidly evaluate the optimal processing conditions for extrusion of polystyrene nanocomposites, and (2) a comparison of a new rapid Cone calorimetry method to conventional Cone calorimetry, and to the gradient heat-flux flame spread method.

2. Experimental[1]

2.1. Extrusion

Homogeneous samples containing organic modified layered silicate (OLS, dimethyl, di-(hydrogenated tallow) ammonium montmorillonite, Cloisite 15A, from Southern Clay Products, www.nanoclay.com) in polystyrene (PS, Styron 663, Dow Chemical) were produced in our twin screw extruder at various screw speeds (B&P, 19 mm, 25:1 L:D, feed rates (2–3) kg/h, feeding zone 170°C, mixing zones (1–4) 190°C). A two hole die produced two 4 mm strands, which were air cooled with an air-knife, and rolled into flat strips (7 mm wide and 2 mm thick, see Fig. 3) using a stainless steel roller attached to the conveyor belt.

2.2. Flammability properties

Homogeneous composition PS samples were evaluated using a new rapid Cone calorimeter procedure and using the flame spread in a *gradient* flux environment (see Fig. 5) in our modified flooring-radiant-panel device (see Fig. 4) . The Rapid Cone procedure used extruded strips (7 mm wide by 3 mm deep by 90 mm long) cut from the strips extruded from the twin-screw extruder. Strips were placed in stainless-steel foil pans (12 mm by 8 mm by 100 mm). Samples were exposed to a fire-like

[1] This work was carried out by the National Institute of Standards and Technology (NIST), an agency of the U.S. government and by statute is not subject to copyright in the United States. Certain commercial equipment, instruments, materials or companies are identified in this paper in order to adequately specify the experimental procedure. This in no way implies endorsement or recommendation by NIST. The policy of NIST is to use metric units of measurement in all its publications, and to provide statements of uncertainty for all original measurements. In this document however, data from organizations outside NIST are shown, which may include measurements in non-metric units or measurements without uncertainty statements.

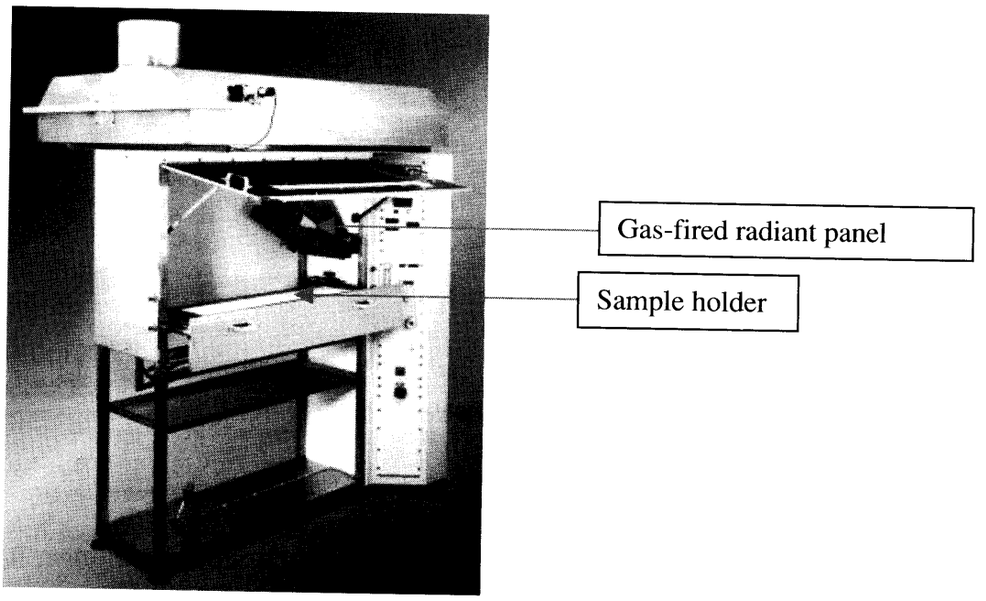

Figure 4 Flooring radiant panel apparatus.

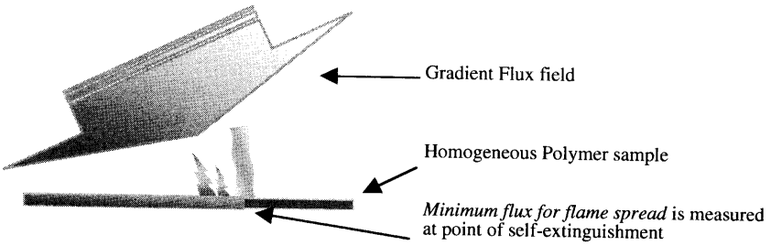

Figure 5 Schematic drawings of the Gradient Flux flame spread approach, where the homogenous sample strip is exposed to a gradient in the flux intensity. The samples are lit on the high-flux end, and allowed to burn until the sample self-extinguishes. The flux at that point is defined as the minimum flux for flame spread (MFFS).

flux of 35 kW/m^2. Standard oxygen consumption calorimetry [33] was performed in a continuous fashion while samples were inserted, burned and removed.

2.3. NMR spectroscopy

NMR measurements were conducted using a Bruker Avance 300 spectrometer operating at 7.05 T. Proton spectra, at 300 MHz, were obtained using a low proton-background probe manufactured by Doty Scientific of Columbia, SC. The magic angle spinning (MAS) frequency used was 2.5 kHz. Bloch-decay spectra were obtained using a 90° pulse width of 1.5 μs and a 2 μs dead time. Proton longitudinal relaxation times, T_1^H, were measured via the inversion-recovery method [35] using direct proton observation. The delay time, τ_{null}, was identified where initially magnetization passed through zero on its way back to the Boltzmann equilibrium level and a lower limit for T_1^H, the longitudinal proton relaxation time, was calculated via the relationship $T_1^H = \tau_{null}/\ln 2$ [36].

3. Results and discussion

3.1. Solid-state NMR of PS/layered-silicate nanocomposite

To demonstrate the effectiveness of the HT system, extrusion was coupled with solid-state NMR characterization to rapidly evaluate the optimal processing conditions for polystyrene (PS) LS nanocomposites.

Many of the properties associated with polymer LS nanocomposites are a function of the extent of exfoliation of the individual silicate sheets (Fig. 6). Barrier properties, modulus, transparency and toughness have all been shown to be directly proportional to the degree of exfoliation, or the quality of the nano-dispersion [37].

Our work, and that of other's, has shown that a careful balance must be found between maximum exfoliation and degradation [26, 38]. Thus, the correct processing conditions must be found that exfoliate the LS, but do not cause too much degradation of either the polymer, or the treatment applied to the LS. We recently developed

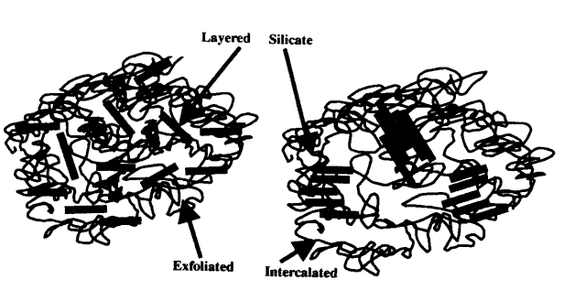

Figure 6 Illustration of exfoliated and intercalated polymer layered-silicate nanocomposite morphologies.

a new method, using solid-state NMR, to quantitatively measure the degree of exfoliation in PA-6 LS nanocomposites based on MMT clay [26].

This method has been streamlined and applied to PS nanocomposites [31]. This method is based on the effect of paramagnetic Fe^{+3} (present in MMT in the central octahedral layer) on the T_1^H of protons near the MMT surface. This paramagnetically induced relaxation directly shortens the T_1^H of protons within about 1.0 nm of the MMT surface. Spin-diffusion allows this relaxation mechanism to propagate into the bulk of the polymer. The extent of this effect on T_1^H depends on both the Fe and MMT concentration, and most importantly, on the average distance between MMT layers. The better the mixing of MMT with the polymer on the nm scale the shorter T_1^H [26].

As stated above the initial proof of the effectiveness of this technique, for quantitative measurement of the average degree of nano-mixing, was demonstrated in PA-6/MMT nanocomposites. To expand the method to PS we first evaluated PS and PS/MMT nanocomposites that had been well characterized by TEM and XRD. This study used a pure PS, and three PS/MMT nanocomposites, which contained the exact same source of MMT; in each case the MMT was treated with a different "onium" salt. The different treatments afforded different nano-mixing. All samples were prepared by free radical polymerization in the bulk. The data in Table II show how the method allows differentiation between PS/MMT nanocomposites that range from an exfoliated to an intercalated morphology. The T_1^H of pure PS is 1.68 s. The PS/P-16, an intercalated material by TEM and XRD, has a T_1^H of 1.47 s. TEM of this sample shows good nano-dispersion of intercalated, multilayer stacks (tactoids) of individual MMT layers that range from 3–10 layers in size. The PS/OH-16, a mixture of intercalated and exfoliated morphologies, has a T_1^H of 1.26 s. TEM of this intercalated/exfoliated sample shows good nano-dispersion of individual MMT layers and tactoids that range from 3–8 layers in size. Finally, the PS/VB-16, with an well dispersed, exfoliated structure has a T_1^H of 1.12 s.

3.2. Processing PS/layered-silicate nanocomposite

With these definitive results in hand, we applied the NMR method to a study of the processing of PS/MMT nanocomposites via twin-screw extrusion. PS was compounded with organic modified layered silicate, 15A. Seven loadings (2%, 3%, 4%, 5%, 6%, 7% and 8% mass fraction) were prepared at four different screw speeds (250 rpm (26.2 rad/s), 300 rpm (31.4 rad/s), 350 rpm (36.7 rad/s), 400 rpm (41.9 rad/s) and 450 rpm (47.1 rad/s)). These 28 runs were replicated 4 to 5 times each in a random fashion. These extrusion experiments (~130) took 2 to 3 days. The NMR characterization of this library (28 samples) was completed in about 3 days. If TEM were required to characterize this 28 sample library it would take 2–3 weeks.

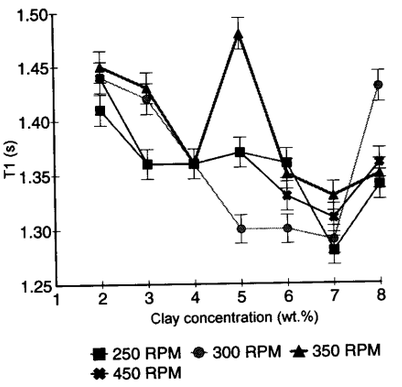

Figure 7 T_1^H for the 28 samples in the processing library. The uncertainty (σ) in T_1^H is 0.05 s.

This factor of 5 to 10 improvement in productivity approaches our goal of characterizing the nanocomposites as fast as the extruder makes them. An added bonus of this NMR method compared to TEM, aside from the speed of analysis, is the quantitative and bulk nature of the measurement.

Fig. 7 shows the T_1^H data for the PS/MMT (15A) nanocomposites. All the T_1^H data fall in between 1.28 s and 1.48 s. The expected decrease in T_1^H with increasing MMT concentration is observed for 26 of the 28 nanocomposites. T_1^H depends on both the MMT concentration and the nano-mixing; thus, to assess the effect of processing conditions on nano-mixing, the comparison must be done between samples within the same MMT loading. The 2 samples which have the poorest dispersion (of the samples within their same MMT loading) are the sample with 5% MMT, processed at 350 rpm, and the sample with 8% MMT, processed at

TABLE II NMR, XRD and TEM characterization of model PS/MMT nanocomposites

Polymer[a]	Layered-silicate	T_1^H (s)	*d*-spacing (nm) from XRD[b]	Change in *d*-spacing (nm)	TEM[b]
PS	–	1.68	–	–	–
–	P-16	–	3.72	–	–
PS/P-16	–	1.47	4.06	0.34	Nano-dispersed, intercalated
–	OH-16	–	1.96	–	–
PS/OH-16	–	1.26	3.53	1.57	Nano-dispersed, intercalated/exfoliated
–	VB-16	–	2.87	–	–
PS/VB-16	–	1.12	No peak	–	Exfoliated

[a]All samples bulk polymerized. P-16 is *n*-hexadecyl triphenylphosphonium MMT; OH-16 is N,N-dimethyl-*n*-hexadecyl-(4-hydroxymethylbenzyl) ammonium MMT, and VB-16 is N,N-dimethyl-*n*-hexadecyl-(4-vinylbenzyl) ammonium MMT. [b]Data from reference [39], mass fraction of organo layered silicate 5%. Uncertainty (1σ) in T_1^H is ±0.05 s.

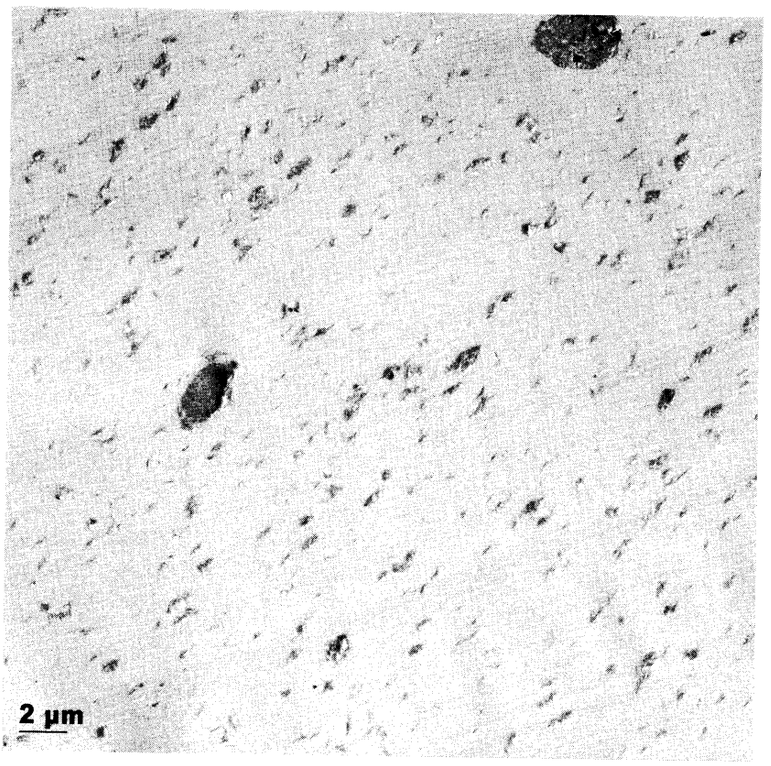

Figure 8 Low magnification TEM of PS/MMT (5% MMT) extruded at 300 rpm.

300 rpm). However, for the remainder of the library, the differences between T_1^H s, within a given concentration, are relatively small. Comparison of the T_1^H data for PS/MMT (15A) extruded with 5% MMT to those for the model PS/MMT (5% MMT) nanocomposites (Table II), discussed above, reveals the following ranking in the quality of nano-dispersion: 300 rpm > 250 rpm = 450 rpm > 350 rpm. Obviously, there is no clear trend between the processing conditions (for the 5% MMT samples) and nano-dispersion. These observations are also true for the rest of the library, i.e., the differences in T_1^H are relatively small, and the degree of nano-mixing is insensitive to the processing conditions used here. All of the processing conditions appear to give nanocomposites with nano-morphologies that range from intercalated (for larger T_1^H) to a mixed intercalated/exfoliated morphology (for smaller T_1^H). Careful inspection of TEM data (not shown) for all 8 extruded PS/MMT (15A) samples, which contain mass fractions of 3% and 5% MMT reveals no discernable difference in the nano-dispersion by TEM. Typical TEM data for this set of nanocomposites is shown in Figs 8 and 9. Although we are not able to identify processing conditions that consistently give the greatest nano-mixing, the additional information NMR supplies makes it an excellent "screening tool" and it is an excellent compliment to the other nanocomposite characterization tools. In addition to the above attributes the NMR method also allows one to determine the extent of degradation of the alkyl ammonium treatment on the MMT surface. In previous work on extrusion of PA-6 with 15A we found at long residence times (240°C, 3 min) up to 80% of the treatment had degraded into tertiary amine [26]. We observed no degradation of the treatment here, presumably due to the lower temperature of extrusion of the PS (170°C).

From the foregoing we conclude that, the NMR—T_1^H characterization method supplies a relatively HT technique for measuring an important attribute associated with MMT-based nanocomposites, i.e., nanoscale mixing of the MMT layers. Furthermore, the optimal processing conditions for PS/15A nanocomposites appear to lie outside the 2-dimensional (%-MMT vs. screw speed) property space that was investigated here. From other work in our laboratories we have found

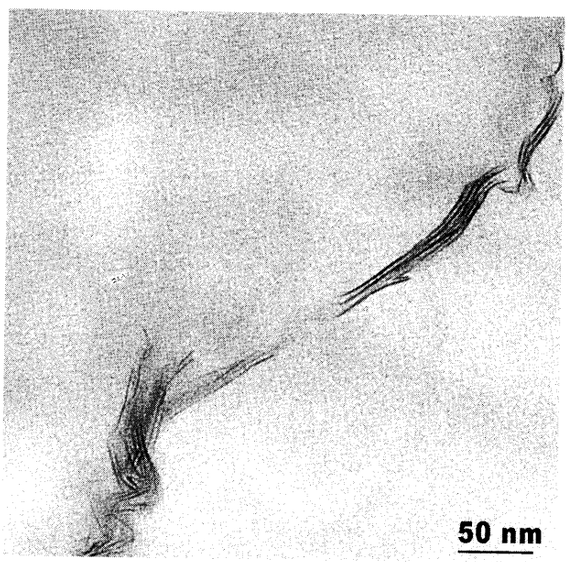

Figure 9 High magnification TEM of PS/MMT (5% MMT) extruded at 300 rpm.

that shorter residence times, or higher screw speeds, can help minimize degradation of the alkylammonium treatment on the MMT. Since for most of the library the 450 rpm processing conditions gave the best, or second best, nano-mixing one could recommend this condition for further study, at least for this polymer and nano-additive combination.

Above, we have compared a new HT material characterization tool (NMR) with a conventional material characterization tool, TEM (see Fig. 1). However, methods are also required for characterization of physical properties, such as mechanical properties and, for our interests, flammability properties. For HT determination of modulus we utilize nanoindentation. Recently, Beake and coworkers have successfully used this technique to characterize the hardness, modulus and creep resistance of polyethylene MMT nanocomposites [40]. The results we have obtained will be reported in a separate manuscript [41].

In the next section the results of modifying the standard flammability characterization tool, the Cone calorimeter, are presented.

3.3. Rapid cone calorimetry

Our interest in nanocomposites is focused on nanostructure, mechanical properties and flammability properties. The traditional approach to evaluating flammability often involves injection molding coupons and testing using standard flammability procedures (UL94 [32], Cone Calorimeter [33], etc.). A significant challenge is to develop HT methods to characterize the flammability of polymers. We save time by directly extruding the test strips. Recently, we have developed several new flammability characterization techniques involving measurement of flame spread and self-extinguishment. Elsewhere, we have reported on these methods, which utilize *gradients* in either the fire environment (heat flux gradient, Fig. 5) or a gradient in the sample composition along the length of the strip [34].

Here we present the results from a new rapid Cone calorimetry procedure. A comparison is made between the new rapid Cone calorimetry method and both the conventional Cone calorimetry, and the gradient heat-flux, flame spread method.

The standard Cone calorimetry test, ASTM 1354, involves burning a polymer sample (100 mm by 100 mm by 25 mm thick) under the influence of a radiant fire-like flux from the cone shaped electric heating element. Combustion products (smoke, carbon monoxide, CO_2, etc.) are analyzed in a hood system. The primary measurement is a determination of the amount of O_2 that has been consumed while burning the sample. This is measured continuously during the experiment, and is referred to as oxygen-consumption calorimetry. Each experiment typically takes 30 min to 90 min.

Fig. 10 shows the schematic drawing representing the steps involved in this rapid Cone calorimetry method. First, test strips are directly extruded instead of injection molding each individual formulation. A second modification is to use much smaller samples than the standard one. Here, the extruded strip is sectioned and used directly. Typical strips are 90 mm long by 7 mm wide by 3 mm thick. The rapid cone samples are cut: either from a several meter long gradient-sample, which contains a gradient in additive composition along the extrusion direction (0% to 10% over a 3 m length), or from a series of homogenous samples extruded one after another. The third modification we make is to keep taking data continuously throughout the burning of all the samples in a series (library). This saves time relative to the normal procedure where each sample is allowed to cool in the calorimeter for several minutes following each test.

Fig. 11 shows data taken on similar sets of PS and PS/MMT samples, using the rapid Cone method and the standard Cone method. The same trend is seen in both data although the absolute values are not the same for the PS/MMT samples. This may be due to a thickness effect; the Rapid Cone samples are 3 mm thick whereas the standard Cone samples were 8 mm thick.

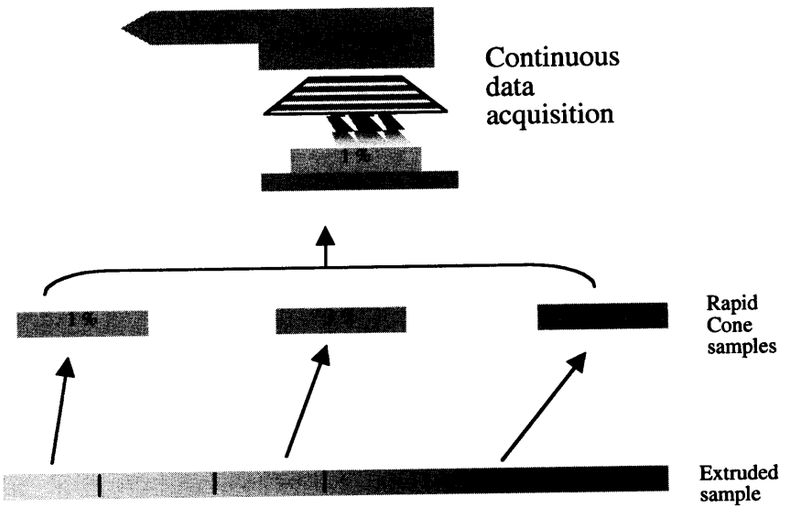

Figure 10 Schematic of rapid cone method.

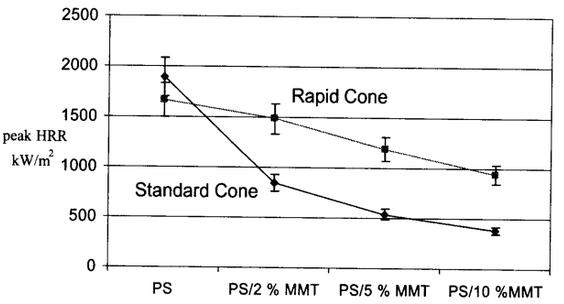

Figure 11 Comparison of Rapid Cone to Standard Cone peak heat release rate (HRR) data. The uncertainty (σ) in the peak HRR is $\pm 10\%$.

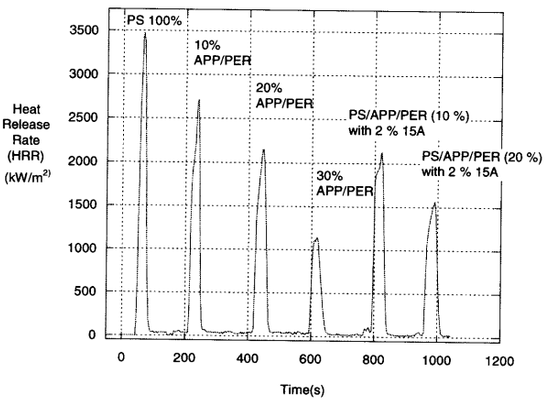

Figure 12 HRR data for 6 PS formulations taken over a 20 min time period.

Fig. 12 shows the data for PS and 5 other PS formulations. This data took 20 min to gather and shows excellent agreement with results from the gradient-flux flame-spread method. The flame spread data is shown in Fig. 13.

A comparison of the data from each method for samples run under both conditions is shown in Fig. 14. The samples evaluated contain a standard intumescent [42] flame retardant combination: a 3:1 ratio of ammonium polyphosphate (APP) and pentaerythritol (PER). Both methods show that the flammability is reduced (MFFS increased, or HRR decreased) as the loading of APP/PER is increased, and both methods show a synergistic, reduction in flammability from the addition of 2% (mass fraction) organo-layered silicate, 15A.

Typically, it takes 2–4 h to gather normal Cone data on 6 samples. Here this was accomplished in 20 min. Combined with the time savings associated with avoiding the injection molding of Cone samples, a factor of 10 improvement is realized using this approach.

The data from the Rapid Cone method is an excellent complement to the Flame Spread date because the Cone also measures ignition time, smoke, carbon monoxide, specific heat of combustion, mass loss rate and a variety of other parameters; all of which are useful in determining the mechanisms which effect flammability. The Flame Spread, or MFFS, measures the interaction of several of these same parameters, which are measured in the Cone. Furthermore, in the flame spread method we measure the self-extinguishing properties

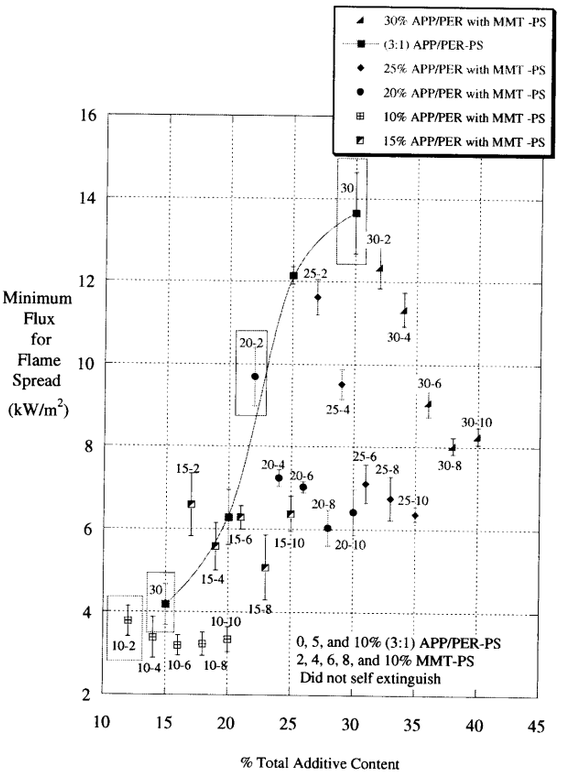

Figure 13 Minimum flux for spread (MFFS) self-extinguishment data for a PS /APP/PER and MMT library. Sample labels (i.e., 10-2) indicate the mass fraction of APP/PER (10%) and the mass fraction of 15A (2%). Samples also evaluated using Rapid Cone (Fig. 12) are: pure PS, PS/10% APP/PER, PS/30% APP/PER, PS/10% APP/PER with 2% MMT (10-2) and PS/20% APP/PER with 2% MMT (20-2). Some are noted in the boxes above. The uncertainty (σ) in the MFFS data is shown by the error bars on the plot. It was determined from 4–5 replicates.

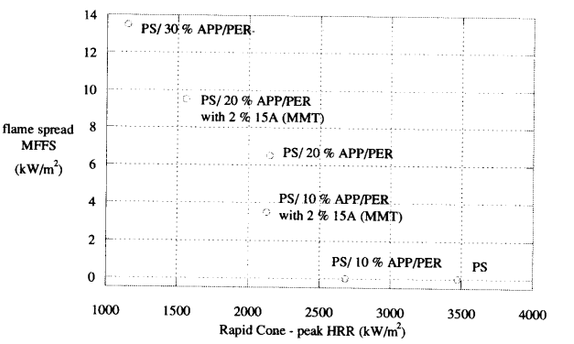

Figure 14 Comparison of Rapid Cone data to Flame Spread data, which reveals the inverse relationship between MFFS and peak HRR. Note: the PS/30% APP/PER is a V-0 rated material in the UL 94 V test [32], and PS and PS/10% APP/PER were non self-extinguishing in the flame spread test (i.e., MFFS = 0). For uncertainty in the measurements see Figs 11 and 13.

of the sample and we plan to relate this to the self-extinguishing behavior seen in the UL94 [32] test.

4. Conclusions

A system of HT methods has been developed for rapid, detailed evaluation of polymers and polymer nanocomposites. The method that combines extrusion with NMR shows a factor of 5 to 10 improvement in productivity,

compared to conventional methods (e.g., TEM) for evaluating two parameters (screw speed, MMT loading) associated with processing of PS/MMT nanocomposites. Unlike many HT "screening" approaches this method prepares real-world scale samples, it uses conventional processing and analytical equipment, and the level of characterization is not compromised; instead it has been enhanced, since the NMR measurement is quantitative and a bulk technique. The method that combines extrusion with Rapid Cone calorimetry also reveals a factor of 10 improvement in productivity, compared to conventional methods (extrusion, injection molding, Cone calorimetry). It too uses conventional processing and analytical equipment, and does not compromise the level of characterization. When combined with the gradient flame-spread method this approach rapidly offers unique flammability property data.

Future work will be focused on expanding the NMR method: (1) to other polymer layered-silicate nanocomposites, (2) to the characterization of degradation of the onium ion treatments on the layered-silicates, and (3) to evaluate the domain size (nano-mixing) of polymer nanocomposites based on other nano-additives (POSS, nano-silica, nano-tubes, etc.). We also will be taking a closer look at the T_1^H method to ascertain the role of O_2 gas equilibration, as well as polymer ageing effects on T_1^H measurements.

Acknowledgements

We thank the following individuals for their assistance with this work: Richard Harris for help with extrusion and injection molding, Walid Awad and Marius Murariu for helpful discussions, and Michael Smith for performing standard Cone calorimetry analysis. We would like to thank the FAA (Interagency Agreement DTFA03-99-X-90009) and the Air Force Office of Scientific Research (ISSA-AFOSR-ISSA-01-0001) for partial funding of this work.

References

1. S. BROCCHINI, K. JAMES, V. TANGPASUTHADOL and J. KOHN, *J. Amer. Chem. Soc.* **119** (1997) 4553.
2. J. C. MEREDITH, A. KARIM and E. AMIS, *Macromol.* **33** (2000) 661.
3. A. P. SMITH, J. F. DOUGLAS, J. C. MEREDITH, E. J. AMIS and A. KARIM, *J. Polym. Sci.: Part B: Polym. Phys.* **39** (2001) 2141.
4. A. KARIM, K. YUREKLI, C. MEREDITH, E. AMIS and R. KRISHNAMOORTI, *Polym. Engin. Sci.* **42** (2002) 1836.
5. M. PETRO, A. SAFIR, R. B. NIELSEN, G. C. DALES, E. D. CARLSON and T. S. LEE, U.S patent no. 6,260,407.
6. J. C. MEREDITH, A. KARIM and E. AMIS, *MRS Bulletin* **27** (2002) 330.
7. K. A. CARRADO, *Appl. Clay Sci.* **17** (2000) 1.
8. M. ALEXANDRE and P. DUBOIS, *Mater. Sci. Eng. (R)* **28** (2000) 1.
9. Y. KOJIMA, A. USUKI, M. KAWASUMI, A. OKADA, Y. FUKUSHIMA, T. KURAUCHI and O. KAMIGAITO, *J. Mater. Res.* **8** (1993) 1185.
10. (a) P. B. MESSERSMITH and E. P. GIANNELIS, *J. Polym. Sci. A., Polym. Chem.* **33** (1995) 1047; (b) A. OKADA, Y. FUKUSHIMA, M. KAWASUMI, S. INAGAKI, A. USUKI, S. SUGIYAMA, T. KURAUCHI and O. KAMIGAITO, US Patent no. 4,739,007.
11. J. W. GILMAN, T. KASHIWAGI and J. D. LICHTENHAN, *SAMPE Journal* **33** (1997) 40.
12. J. W. GILMAN, T. KASHIWAGI, S. LOMAKIN, E. GIANNELIS, E. MANIAS, J. LICHTENHAN and P. JONES, in "Fire Retardancy of Polymers: The Use of Intumescence," edited by M. Le Bras, G. Camino, S. Bourbigot and R. Delobel (The Royal Society of Chemistry, Cambridge, 1998) p. 203.
13. J. W. GILMAN, *Appl. Clay. Sci.* **15** (1999) 31.
14. J. W. GILMAN, C. L. JACKSON, A. B. MORGAN, R. H. HARRIS, E. MANIAS, E. P. GIANNELIS, M. WUTHENOW, D. HILTON and S. PHILLIPS, *Chem. Mater.* **12** (2000) 1866.
15. E. P. GIANNELIS, *Adv. Mater.* **8** (1996) 29.
16. R. A. VAIA, G. PRICE, P. N. RUTH, H. T. NGUYEN and J. D. LICHTENHAN, *J. Appl. Clay Sci.* **15** (1999) 67.
17. H. FONG, R. A. VAIA, J. H. SANDERS, D. LINCOLN, A. J. VREUGDENHIL, W. D. LIU, J. BULTMAN and C. G. CHEN, *Chem. Mater.* **13** (2001) 4123.
18. J. D. LICHTENHAN, N. Q. VU, J. A. CARTER, J. W. GILMAN and F. J. FEHER, *Macromol.*, **26** (1993) 2141; J. D. LICHTENHAN, J. W. GILMAN, I. M. K. ISMAIL and M. BURMEISTER, *J. Chem. Mater.* **8** (1996) 1250.
19. Z. AHMAD and J. E. MARK, *Chem. Mater.* **13** (2001) 3320.
20. H. L. FRISCH and J. E. MARK, *ibid.* **8** (1996) 1735.
21. F. M. UHL, F. J. LAMELAS and C. A. WILKIE, *Abstr. Pap. Amer. Chem. S.* 220: 66-PMSE Part 2 Aug 20 (2000).
22. Z.-H. LIU, Z.-M. WANG, X. YANG and K. OOI, *Langmuir* **18** (2002) 4926.
23. P. M. AJAYAN, L. SCHADLER, C. GIANNARIS and A. RUBIO, *Adv. Mater.* **12** (2000) 750.
24. T. K. KASHIWAGI, E. GRULKE, J. HILDING, R. HARRIS, W. AWAD and J. DOUGLAS, *Macromol. Rapid Comm.* **2** (2002) 761.
25. For a Description of the POSS Materials Available See: www.hybridplastics.com
26. D. L. VANDERHART, A. ASANO and J. W. GILMAN, *Chem. Mater.* **13** (2000) 3796.
27. For Example: Equipment by Bruker for High Throughput Screening of Combinatorial Libraries Using X-ray is Discussed at: www.bruker-axs.de.
28. C. L. THOMAS and A. J. BUR, *Polym. Engin. Sci.* **3** (1999) 1619.
29. A. J. BUR, S. C. ROTH and M. MCBREARTY, *Rev. Sci. Instr.* **73** (2002) 2097.
30. D. L. VANDERHART, A. ASANO and J. W. GILMAN, *Macromol.* **34** (2001) 3819.
31. S. BOURBIGOT, J. W. GILMAN and D. VANDERHART, manuscript in preparation.
32. UL 94: The Standard for Flammability of Plastic Materials for Parts in Devices and Appliances. www.ul.com/services/flame.html
33. V. BABRAUSKAS and R. D. PEACOCK, *Fire Safety J.* **18** (1992) 255.
34. M. NYDEN, J. W. GILMAN, R. DAVIS and J. R. SHIELDS, *SAMPE* (2002) 738.
35. T. C. FARRAR and E. D. BECKER, "Pulse and Fourier Transform NMR" (Academic Press, New York, 1971) p. 20f.
36. This relationship assumes full initial inversion of the magnetization and single-exponential recovery. The paramagnetic contribution to T_1^H originating from the MMT clay produces slightly accelerated early decay relative to the typically exponential behavior seen at longer times; hence, this relationship yields a lower limit to the T_1^H that would describe the longer time behavior.
37. M. ALEXANDRE and P. DUBOIS, *Mater. Sci. and Eng. (R)* **28** (2000) 1.
38. H. R. DENNIS, D. L. HUNTER, D. CHANG, S. KIM, J. L. WHITE, J. W. CHO and D. R. PAUL, *Polymer* **42** (2001) 9513.
39. J. ZHU, A. B. MORGAN, F. J. LAMELAS and C. A. WILKIE, *Chem. Mater.* **13** (2001) 3774.
40. B. D. BEAKE, S. CHEN, J. B. HULL and F. GAO, *J. Nanosci. Nanotech.* **2** (2002) 73.
41. R. DAVIS and J. W. GILMAN, manuscript in preparation.
42. S. BOURBIGOT and M. LE BRAS, in "Fire Retardancy of Polymers: the Use of Intumescence," edited by M. Le Bras, G. Camino, S. Bourbigot and R. Delobel (The Royal Society of Chemistry, Cambridge, 1998) p. 223.